Journal of Ocean Engineering and Technology, Vol. 1, No. 2, pp. 215~227, December, 1987

⊙ Technical Paper

Dynamics of Disconnected Risers under Rigid and Compliant Hang-off+

D. Y. Yoon* and N. M. Patrikalakis**

강성 및 컴플라이언트 행오프 하에서의 미연결송유관의 동력학

윤 덕 영 · 엔. 엠. 패트리카라키스

Key Words : Riser(석유시추보호관), Finite Different Method(유한차분법), Dynamic Buckling Type Response(동적 좌굴형 반응), Support Platform(지지플랫폼)

초 록

석유시추 보호관의 비선형 운동을 시뮬레이트하는 유효한 해법이 non-uniform grid 유한차분법과 implicit time 적분법에 근거하여 제시되었다. 극한 상태에 있는 지지 플랫폼의 상승 가속도에 의해 생기는 보호관의 동적 좌굴형 반응에 관하여 상세히 연구되었고, 이 반응에 미치는 중요 변수가 규명되었다. 운동의 현저한 감소와 이에 따른 응력들이 컴플라이언트 행오프(hang-off)를 적용시킴으로써 얻어졌다.

1. Introduction

Deep water risers disconnected at the wellhead and suspended freely from the surface support platform may suffer from large dynamic tension variation arising from extensional resonance or a large downward heave acceleration exceeding the free-fall acceleration of the riser system. Tension provides most of the flexural rigidity in risers and, therefore, large tension variation may lead to dynamic buckling and very large bending stresses in addition to large tension stresses. In order to study these large coupled, possibly resonant, axial and flexural motions of hanging riser system, a non-linear model is employed.

Solution methods for formulating and above general non-linear problem can be classified into three major categories; the finite element method, the finite difference method and the spectral method. Ref. (19) solves the structurally linearized riser equations in the time domain using a centered finite difference scheme and Newmark's method for time integration. His solution employs an expeimental 2-D flow model for the prediction of the non-linear hydrodynamic forces. Ref. (7) presents a three-dimensional large deflection finite element

+ Presented at the 1987 KCORE Autumn Conference

* Member, Dae Woo Shipbuilding & Heavy Machinery Co., Ltd., Korea

** Massachusetts Institute of Technology, USA

model of an inextensible rotationally uniform elastic rod without torque. The first order Adams-Moulton method is used for time integration. Ref. (4) presents a finite element model for deep ocean mining pipes and simulates non-linear transient motions in the time domain.

Up to quadratic terms in the extensional strain-displacement relation are used. A linear three step method is employed for time integration. The effect of drag cofficient on the response characteristics of the lower end of the pipe is also studied. Ref. (11) simulates the motions of connected risers in the time domain using the natural mode expansion method. Second order geometric non-linear terms for the tension displacement relation and non-linear fluid drag forces are retained in his formulation. Time integration is performed using an explicit scheme. Ref. (16) deals with inextensible and rotationally uniform slender elastic rods with torque applied at the ends. His solution method is based on a finite difference approximation of space derivatives and a semi-explicit time integration method. The condition for numerical stability is given in term of the ratio of the time step to the space grid size. Ref. (17) derives the basic equations for small amplitude vibrations of a marine riser with equal principal stiffnesses retaining a second order non-linear tension-displacement relation and non-linear fluid forces. Spatial discretization is performed using a hybrid finite element method. The implicit Houbolt method is employed for time integration. Ref. (2) simulates the non-linear motions of single span mooring lines by expanding the cable motions in the natural modes of the problem. Analytical asymptotic evaluation of the natural modes was achieved and compares well with numerical calculations. Ref. (3) carries out simulations of shallow sag cables by expanding the cable motions in two different sets of orthogonal functions, first, the natural modes and, second, sinusoids. It is found that sinusoidal expansions are preferable to natural mode expansions in the simulation of elastic type waves since a large number of natural modes are required to accurately model elastic traveling wave solutions. Ref. (26) simulates non-linear vibrations of an elevating pipeline. Spatial derivatives are replaced by finite difference analogues and the resulting initial value problem for a system of ordinary differential equations is integrated in the time domain using an implicit scheme. Ref. (18) examines the lateral dynamics of freely hanging production risers. The finite element method for spatial discretization and Newmark's method for time integration are employed. Geometric stiffness nonlinearities up to second order in the displacements are accounted for.

Time domain simulation for a shallow water riser due to surge motion only is presented. Considering the riser lengths and the time steps used, extensional wave type solutions and heave effects were not investigated. Ref. (14) presents a finite element model for the analysis non-linear coupled dynamic axial and lateral motions of a hanging riser. Up to quadratic terms in the tension-displacement relation are used. Simulation of a 1.2*km* hanging riser response to heave and surge motions with current and wave excitation is carried out. Time integration is performed using the Houbolt method. The response to a random wave input is also presented. Extensional wave solutions and negative total effective tension effects were not studied. Ref. (14) identified substantial differences in computations of bending stresses near the top end of the riser due to variations in available solution procedures and wave loading in extreme wave excitation. The region very close to the top end of the riser was found to be the most highly stressed for the riser design and excitation conditions studied. A related problem of dynamic buckling of vertical hanging strings due to parametric excitation arising from heave motion of the top end has been studied in Ref. (10) using linearized equations except for the effect of fluid drag and a modal expansin solution method. It was found that for small tension variations, to which the analysis of Ref. (10) is limited, the straight configuration is unstable for certain values

of the excitation frequency. For the cases studied in Ref. (10) the ultimate lateral response is very small in water due to significant drag, while it becomes very significant in air.

Review of the above references revealed that the solutions of the governing equations of hanging risers involving large coupled axial and lateral motions in the presence of compressive axial forces, anticipated in the rigid hang-off mode under extreme enviornmental conditions, have not been studied. The natural mode expansion method does not appear to be attractive in the simulation of these large motions because it is computationally difficult to determine the natural modes of motions around a nominal static configuration in the presence of extensional waves. In addition, modal expansions may require a large number of terms in the case of high frequency excitation of long risers in the presence of current because lateral motions are expected to decay rapidly away from the top end. The sinusoidal expansion method is also not very attractive in the simulation of the problem addressed here because of the presence of sharp boundary layers in bending momenta and shear forces. Other spectral expansion methods, such as those based on Chebychev polynomials, are expected to alleviate such a difficulty, but are complex to implement[8]. The solution scheme adopted in this paper is based on a nonuniform grid finite difference space derivative discretization. The method employed has some highly desirable properties in the problem at hand, such as an automatic adaptive mesh capability and a deferred correction capability. The adaptive mesh, which is created automatically based on equidistribution of discretization errors, efficiently resolves the steep changes of bending moment and shear force. The deferred correction capability provides a higher order finite difference approximation whenever necessary at reasonable computational expense. The solution scheme adopted has been proposed for the solution of complex nonlinear two-point boundary value problems for ordinary differential equations which involve rapid localized variations in the solution[23]. Particular emphasis is placed on the study of dynamic buckling type responses of hanging risers due to extreme excitation conditions. Numerical results suggest that the concept of compliant hang-off is quite useful in improving the responses of hanging riser systems and reducing the stress level significantly.

2. Problem Formulation

A mathematical model for the static behavior of slender elastic rods undergoing large deformations with small strains is given in Ref. (12) and (13). The modifications to account for dynamic effects and the presence offluid inside and outside a tube modelled as a slender rod can be found in Ref. (17) and (19). Ref. (21) extended the mathematical model derived in Ref. (17) and (19) to allow the computation of the motion of a compliant riser modelled as a nonrotationally uniform slender elastic rod with space varying torque. The assumptions made in modelling of the global static and dynamic behavior of riser systems are summarized below.

The riser is modelled as a thin rod rather than as a shell. This assumption is acceptable since we are only interested in the global behavior of the system and the diameter to length ratio is very small. The material is assumed to be homogeneous and isotropic which is a good model for steel structures. Although deformations may become large, strains are assumed to remain uniformly small. This permits the use of linear constitutive relations between stresses and strains. Shearing deformations are neglected. This implies that cross sections remain planar after bending and normal to the neutral axis as in the Rayleigh slender beam theory[5]. This assumption is realistic as long as the order of the highest flexural mode excited is much smaller than the length to diameter ratio. This is valid for the problem at hand. Finally, thermal effcets are neglected.

Consistent with the objectives of this paper, dealing with extreme envioronmental excitation conditions of a drilling riser in a disconnected mode, the following additional simplifications are

introduced. First, the riser is assumed to be rotationally uniform which is a good approximation for steel drilling risers[17]. The mass per unit length in the tangential direction ζ, $m\zeta$, is also assumed to be same as that in the other two principal directions, m[1]. This implies that the internal fluid essentially moves with the riser in the tangential direction just as it does in the lateral direction. This approximation can be made as long as the lower end of the riser can be considered closed and axial motions are much larger than axial extensions. Next, all external forces from currents, waves, support vessel motions and the response of the riser are assumed to lie on a single vertical plane. This approximation is likely to exaggerate the environmental loads and the resulting stresses because all major excitations are concentrated in a single plane. In addition, waves and support vessel motions are assumed to be monochromatic. These assumptions are adopted because of the extreme environmental conditions appropriate for a survival analysis of hanging risers over short time intervals. Slow horizontal platform oscillation due to second order drift forces may be treated as currents when their frequencies are sufficiently below the first flexural natural frequency of the riser. This is true for short and medium water depth. For deeper water, slow drift oscillation may excite the first few natural modes. In such cases the ratios of the diameter and of the slow drift motion amplitude to the flexural wave length are small and, therefore, the resulting stresses due to drift effects are expected to be small as compared to the maximum stress due to other effects. Finally, rotational inertia terms are neglected in the moment equations because the ratio of the excited flexural mode wave length to diameter is very large. This assumption simplifies the governing equations to the Euler beam approximation[5], which is commonly used in riser analysis[17,19]. In addition, structural damping forces are neglected from the equations of motion. The structural damping force in the normal direction is known to be very small as compared to the hydrodynamic damping force in the same direction. The contribution of the structural damping force in the axial direction to the overall damping force in that direction is expected to be larger and, therefore, its omission is likely to exaggerate the dynamic tension magnification near resonance. It is well known that when current, wave and applied horizontal oscillation of the upper end of a riser are in the same plane, out-of plane (lift) response is normally present[19].

The frequency and amplitude characteristics of lift motion vary significantly with the parameters of the imposed flow as suggested by the small scale experiments found in the above. Ref. (19). No general rational models are, however, available to compute lift and drag response for the excitation conditions described above. For the special case of uniform current excitation, a model for lift and mean drag response prediction, based on strip theory and rigid cylinder experimental data exists and compares well with experimental data from a small scale riser experiment[20]. Its extension to the sheared current case can be found in Reg. (22).

For current excitations and medium to deep water risers, stresses due to lift motion are expected to be small compared to the maximum stresses due to in-plane response in a survival excitation condition. Vortex induced lift response may be important in low amplitude-long term fatigue life estimates. As indicated in the above Ref. (22), however, one of the major effects of lift response is to increase mean drag parallel to the current. Unfortunately, it is not known at present how to estimate the effects of lift response on the in-plane forces for cases other than constant current excitation. A promising new approach to rationally compute the forces on circular cylinders in viscous flows can be found in Ref. (27).

Based on the above assumptions, the general equations of planar motion can be easily derived from the general equations of motion of compliant risers[2].

$$T_s - Q\Omega - W \sin \phi + F_H^{\zeta} = ma^{\zeta} \tag{1}$$

$$Q_s + T\Omega - W \cos \phi + F_H^{\zeta} = ma^{\zeta} \tag{2}$$

$$(EI\Omega)_s + Q = 0 \tag{3}$$

$$\phi_s = \Omega \tag{4}$$

$$x_s = (1+e)\cos\phi \tag{5}$$
$$y_s = (1+e)\sin\phi \tag{6}$$
$$v^{\zeta}{}_s = \Omega v^{\xi} + e_t \tag{7}$$
$$v^{\xi}{}_s = -\Omega v^{\zeta} + (1+e)\omega \tag{8}$$

where,

$$\omega = \phi_t \tag{9}$$
$$a^{\xi} = v^{\xi}{}_t - v^{\zeta}\omega \tag{10}$$
$$a^{\zeta} = v^{\zeta}{}_t + v^{\xi}\omega \tag{11}$$
$$T = EAe - (1-2\nu)(P_o A_o - P_i A_i) \tag{12}$$

Subscripts s and t denote partial derivatives with respect to the arc length of the center line and time. T, W are the effective tension and weight of the riser. Q, Ω are the shear foce and curvature. ϕ is the angle between the horizontal and ζ directions. EI, EA denote bending and extensional rigidity. P_oA_o, P_iA_i denote the hydrostatic pressure forces on the external and internal pipe section. e, ν are the extensional strain of the center line and the Poisson's ratio of the pipe material. x, y are the horizontal and vertical displacements of the center line. v^{ξ}, v^{ζ} are the riser velocities in the tangential and normal directions.

Consistent with the above discussion, the hydrodynamic forces will be estimated using a modified form of Morison's equation[24]

$$F_H^{\xi} = 0.5\rho_w C_f P_e^{\xi} |v_r^{\xi}| v_r^{\xi} + (1+C_m^{\xi}) m_w^{\xi} a_w^{\xi} - C_m^{\xi} m_w^{\xi} a^{\xi} \tag{13}$$
$$F_H^{\zeta} = 0.5\rho_w C_d D_e |v_r^{\zeta}| v_r^{\zeta} + (1+C_m) m_w a_w^{\zeta} - C_m m_w a^{\zeta} \tag{14}$$

where

$$m_w = \rho_w \pi D^2/4$$
$$m_w^{\xi} = \rho_w (A_b - A_o)$$

D is the local outer diameter of the riser and buoyancy modules. A_b is the buoyancy modules outer cross-sectional area. A_b is equal to A_o within the bare part of the riser.

P_e^{ξ} is an equivalent wetted perimeter of the cross-section defined in such a manner so as to account for frictional effects and separation effects due to diameter discontinuities

$$P_e^{\xi} = P^{\xi} + [C_d^{\xi}(A_c - A_o)/C_f L_c] \tag{15}$$

C_f and C_d are a frictional damping coefficient for flows in the tangential direction and a normal drag coefficient, respectively. C_d^{ζ} is a separation and wake formation drag coefficient for the riser connectors (flanges) for flows parallel to ζ. Riser connectors (flanges) are believed to be the primary sources of separation drag in the axial direction[25]. A_c is the frontal area of the connector (flange) and L_c is its length (thickness). P^{ζ} is the overall wetted perimeter of the cross-section.

v_r^{ξ} and v_r^{ζ} are relative velocities of the flow with respect to the riser in the tangential direction, ζ, and the normal direction, ξ, respectively. a_w^{ξ}, a_w^{ζ} are fluid accelerations in the same directions. C_m is the added mass coefficient in ξ direction and C_m^{ζ} is the added mass coefficient in ζ direction due to the presence of the diameter discontinuities.

In order to solve the above equations of planar motion, eight boundary conditions are required together with appropriate initial conditions. At the lower end, force equilibrium on the lower marine riser package (LMRP) and zero curvature, because of the presence of the lower ball joint, lead to three boundary conditions. At the top end, zero curvature, because of the presence of the upper ball joint, is employed. For rigid hang-off, the remaining four condtions are obtained by prescribing motions and velocities of the top end in the vertical and horizontal directions. For compliant hang-off, the vertical boundary conditions are replaced by force equilibrium of the tensioner and the displacement-velocity relation. Detailed derivation of the boundary conditions and, in particular, modeling of forces experienced by the tensioner system and the LMRP can be found in Ref. (29). The solution of the general equations due to time invariant excitations such as current drag, provides initial conditions for the solution of a general dynamic problem. A vertically straight riser configuration can also be used as an initial condition for the dynamic problem. In order to diminish the computing time required to reach the ultimate dynamic response amplitude, the static response to the time invariant excitation is pref-

erable, as an initial condition, to the vertically straight riser configuration. The initial velocities of the riser system may be set to zero.

3. Time Domain Simulation

We solve the mixed initial-boundary value problem involving a system of non-linear partial differential equations by converting it to a sequence of boundary value problems, involving a system of non-linear ordinary differential equations, at each time step. In order to carry out this conversion, we semi-discretize in the time direction first and we, subsequently, solve the resulting boundary value problem very accurately in space using a general non-uniform grid finite difference method for non-linear two-point boundary value problems proposed in Ref. (23). Time derivatives in the boundary conditions are also approximated by their finite difference analogues. It is convenient to introduce a solution vector, S, and solution vector functions G and R so that we may recast the governing equations in the following compact from

$$S_s = G(S) + R(S, S_t) \tag{16}$$

where

$$S = (T, Q, v^\xi, v^\xi, \Omega, \phi, x, y)^T$$

G is the vector function which does not include the time derivatives of the components of the solution vector. R is the vector function which includes the time derivatives of the components of the solution vector.

It is important to discretize stably in the time direction. In fact, an unconditionally stable scheme is desirable because of the fact that very dense space discretization is required near the ends in order to resolve the sharp changes of the solution. For this reason, we choose the Crank-Nicolson method for time integration[6]. Using finite differences to represent time derivatives, the system of first order partial differential equations 16 is converted to an ordinary boundary value problem at time t^n

$$[S_n^s - G(S^n)] + [S^{n-1}{}_s - G(S^{n-1})] = 2R(\Delta S^n/\Delta t^n, (S^n + S^{n-1})/2)$$

and therefore

$$S_n^s = G(S^n) - [S^{n-1}{}_s - G(S^{n-1})] + 2R(\Delta S^n/\Delta t^n, (S^n + \Delta S^{n-1})/2) = F(S^n) \tag{17}$$

where

$$\Delta S^n = S^n - S^{n-1}, \quad \Delta t^n = t^n - t^{n-1}$$

The time derivatives appearing in the boundary equations are replaced by the following second order accurate finite difference analogue

$$S_t{}^n = c^n S^n - c^{n-1} S^{n-1} + c^{n-2} S^{n-2}$$

where

$$C^n = 3/(2\Delta t), \quad C^{n-1} = 2/\Delta t, \quad C^{n-2} = 1/(2\Delta t)$$
$$\Delta t = t^n - t^{n-1} = \text{constant}$$

Now we can proceed in the time integration by solving the ordinary non-linear two-point boundary value problem at each time t^n using the modified Newton's method coupled with deferred correction[15,23]. As stated earlier, a non-nuiform grid finite difference method based on simple trapezoidal rule approximation of equation (17) is used

$$(S_{j+1} - S_j)/h_j = (F(s_j, S_j) + F(s_{j+1}, S_{j+1}))/2$$

where superscript n is omitted and $h_j = s_{j+1} - s_j$ is the mesh spacing which may be non-uniform. The solution at the previous time step, S^{n-1}, is used as an initial guess for S^n, which is a very good approximation and allows rapid convergence of the iterative solution of the boundary value problem.

Two important properties of the method are:

Adaptive mesh: As stated earlier, the discretization mesh is modified automatically in order to equidistribute the discretization error of the finite difference approximation. Because of the adaptive mesh, our numerical scheme deals with the problem at hand very efficiently since the mesh can be made locally finer.

Deferred correction: Using the information obtained during the local error estimation required for the mesh correction, higher order approximations can be obtained efficiently, whenever a tight externally given absolute error is required. Due

to space limitations, the reader is referred to Ref. (23) and (29) for more information.

4. Numerical Application and Results

The principal characteristics of the riser design used as an example in this paper are summarized in Table 1. The characteristics of the LMRP used can be found in Table 2. The characteristics of the excitation condition chosen to illustrate the phenomena of interest in this work are summarized in Table 3. These are representative of extreme environmental conditions likely to be encountered when disconnection of the LMRP from the wellhead becomes necessary. The amplitude of heave and surge motions of the surface support vessel are estimated from the response of a twenty thousand *ton* drillship in head seas. Phase angles are measured with respect to the incident wave elevation at the horizontal position of the riser attachment point on the support vessel. The above riser design and excitation allow us to investigate the situation where large dynamic tension comparable to or greater than the static tension can be generated if the heave excitation is transmitted directly to the riser top under rigid hang-off.

Table 1 Riser principal characteristics

Characteristics	Symbol	Unit	Riser
Total length	L	m	1,500
Outer diameter	D_0	m	0.4964
Inner diameter	D_i	m	0.3747
Extensional rigidity	EA	GN	4.121
Buoyancy module			
Outer diameter	D_b	m	0.7
Joint length	L_{joint}	m	12.192
Number of buoyancy			
Modules per joint	n	ea	1
Buoyancy module			
Length	L_b	m	9.754
Mean effective			
Diameter	D_e	m	0.6413
Mean effective			
Perimeter	P_e^{ζ}	m	5.39
Mean effective weight			
Per unit length	W	N/m	168.3
Mass per unit length:			
Riser steel	m_r	kg/m	229.3
Internal fluid	m_i	kg/m	113.0
Buoyancy module	m_b	kg/m	29.8
Tangential			
Effective mass	m_e^{ζ}	kg/m	424.6
Normal			
Effective mass	m_e^{ζ}	kg/m	530.4

Table 2 LMRP characteristics

Characteristics	Symbol	Unit	Value
Mass	M_L	kg	90,147
Height	H_L	m	4.572
Diameter	D_L	m	3.439
Volume	V_L	m^3	42.475
Wet weight	W_L	kN	457.24
Vertical			
Effective mass	$M_{Le}{}^y$	kg	133,684
Horizontal			
Effective mass	$M_{Le}{}^x$	kg	133.684
Drag area:			
Vertical	A_L	m^2	9.29
Horizontal	S_L	m^2	49.40

Table 3. Excitation condition description

Characteristics	Symbol	Unit	Condition A
Frequency	ω_0	rad/s	0.60
Period	T_0	s	12.57
Amplitude:			
Wave	A_w	m	6.0
Heave	H_0	m	4.8
Surge	S_0	m	1.5
Phase angle:			
Heave	ϕ_H	degrees	0
Surge	ϕ_S	degrees	90
Max. heave			
Acceleration	$a_{\text{vessel}}{}^y$	g	0.176
Linear current:			
at Sea bottom	V_{cB}	m/s	0
at Surface	V_{cS}	m/s	1

As stated earlier, the dynamics of the hanging riser systems depend very much upon effective tension. If tension variation with rigid hang-off is too large to maintain an adequate level of total effective tension, then compliant hang-off may be advantageous. A simplified analysis of axial dynamics of vertical hanging risers can be employed to appropriately choose the tensioner spring constant under such compliant hang-off[29]. The first extensional natural frequency of the riser is 2.62 *rad/s*, which is above significant wave excitation (0.3 *rad/s*~1.4*rad/s*). The excitation fre-

quency of (0.6 *rad/s*) is low enough to allow us to make the assumption of inextensibility. Using the inextensibility assumption for a vertical hanging riser with rigid hang off and neglecting drag forces along the riser and on the LMRP, we estimate the maximum extent of the riser from the lower end, L_{max}, in which effective tension is likely to remain positive

$$L_{max} = (W_L - a_{vessel}{}^y M_{Le}{}^y)/(a_{vessel}{}^y m_e{}^\xi - W)$$

which gives 400*m*, where $m_e{}^\xi$ is the effective mass in the axial direction including added mass and $M_{Le}{}^y$ is the effective mass of the LMRP in the vertical direction including added mass. Therefore, we expect that a substantial fraction of the length of the riser from its top end (1.1*km*) may involve negative effective tension for part of the period of the oscillation. In addition, large lateral loads are expected in the upper part of the riser which is close the support vessel excitation and within strong wave action. Using the static solution in the presence of current excitation as an initial starting configuration, the riser motions are simulated in the time domain for two different top end boundary conditions, rigid hang off and compliant hang off. In our simulations we used a constant value of added mass coefficient $C_m = 0.5$ and two values of drag coefficient $C_d = 0.8$ and 1.2. These estimates of C_m and C_d are based on rigid cylinder experiments involving sinusoidal oscillations parallel to a current or in the absence of current[24,28]. In our calculations a value of $C_f = 0.005$ and $C_d{}^\xi = 0.8$ were used[9]. The above values of the hydrodynamic coefficients are reflected in our calculations of effective mass and effective perimeter of the riser system.

5. Rigid Hang-off

Figure 1 is the plot of the maximum absolute values of the total axial stress along the length expected in one period of oscillation. Axial stress is made up from tension and bending components. This figure indicates that the maximum stress in the riser occurs very close to the top end. By

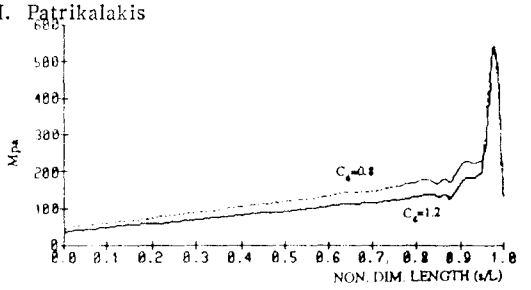

Fig. 1 Max. total axial stress

comparison to the static solution, the maximum stresses are primarily due to dynamic effects and are large enough to endanger the riser system from short term fatigue failure. A qualitative discussion of the phenomena giving rise to such high stresses is attempted below. In order to understand how much tension and bending contribute to the maximum stress, the time traces of tension and bending stresses at the position, where maximum total stress is obtained, are plotted in Figure 2. A Fourier series decomposition of tension and bending stress time traces shown in Figure 2 indicates the importance of non-linear effects in the governing equations of the problem in generating a periodic response which includes significant higher harmonics[29]. The non-monochromatic nature of tension stress is more pronounced than that of bending stress. One of the more important features of Figure 2 is the small magnitude of negative (compressive) tension stress. The heave acceleration of the top end is

$$a^y = -H_0\omega_0{}^2 \sin(2\pi t/T_0)$$

Therefore the acceleration of the top end remains

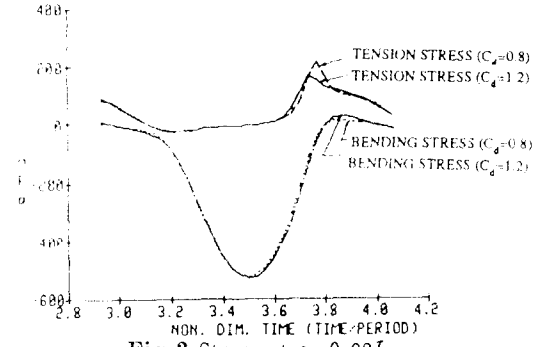

Fig. 2 Stress at $s = 0.98L$

negative in the first half of each period of oscillation. This leads to large negative tension assuming that the riser does not "buckle" laterally.

However, once flexural deformation occurs, compressive axial forces can not increase so much. Instead, the available energy generates large bending deformation and is absorbed by bending strain energy. This is why the tension stress has no sharp negative peaks while sharp positive peaks appear in Figure 2. Another interesting feature observed in Figure 2 is the relative phase of tension and bending stress. When tension is sufficiently positive, bending stress is small in magnitude as is the usual case with properly tensioned risers. However, as total tension decreases and eventually becomes negative, the magnitude of bending stress rapidly increases and reaches an extreme value at about 1/4 period after tension reaches its largest compressive value. Subsequently, as tension rises due to upward acceleration of the surface support platform, bending deformation reduces rapidly reaching its minimum value nearly at the time of maximum tension. This alternating sequence of positive and negative effective tension effectively reduces the flexural rigidity of the giving rise to large bending deformation. It is also worth noting that in this process the effect of lateral drag on the maximum stress is relatively small as can be seen from Figures 1 and 2 and for a 50% change of the drag coefficient. Figures 3 and 4 are plots of effective tension along the length for a series of time instances within one period of oscillation. Effective tension is normalized with the maximum static tension at the top end($0.73MN$). Note that near the upper end, the magnitude of the difference between the maximum tension and static tension is much larger than the difference between the minmum tension and static tension. This is due to the presence of large deformation as explained before. The above total tension figures indicate that tension becomes negative within a significant fraction of the length starting at the top end and for part of the period of oscillation. Figures 5 and 6 are plots of bending stress along the length for a series of time instances within one period of oscillation. Note that although negative tension exists in a substantial region along the length

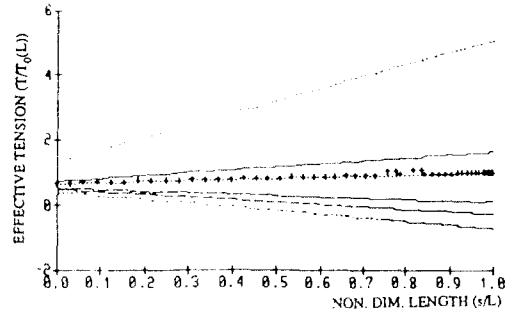

Fig. 3 Effective tension ($C_d = 0.8$)

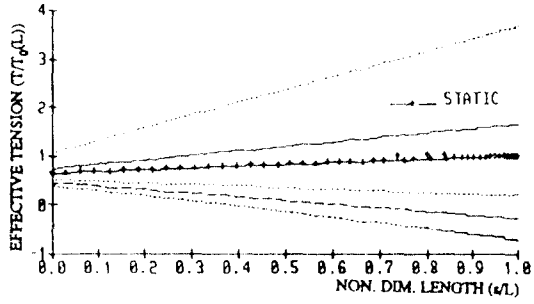

Fig. 4 Effective tesion ($C_d = 1.2$)

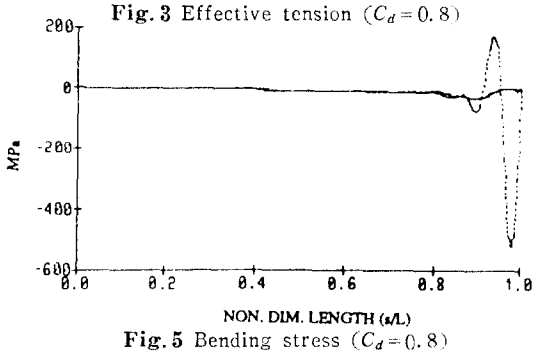

Fig. 5 Bending stress ($C_d = 0.8$)

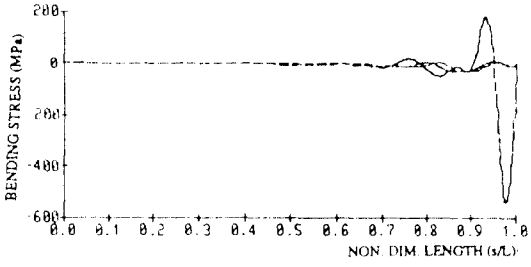

Fig. 6 Bending stress ($C_d = 1.2$)

from the top end, large bending stresses are confined near the top end of the riser. As can be seen from the above pictures lateral oscillation are confined near the top end have a much smaller extent than the region of negative tension measuedr from the top end. This is an interesting result indicating that sufficiently away from the top end the riser behaves as a semiinfinite beam under positive tension. For the amplitudes of lateral oscillation of interest (a few diameters) and in the presence of current, the oscillatory drag is proportional to the oscillatory velocity for most of the length. This results in a linearly damped flexural wave which, because excited wave lengths are small compared to the length, decays to insignificant values within a few wave lengths. A much slower rate decay of flexural waves should be expected in the absence of current because drag is proportional to the square of the oscillatory velocity for the entire length[29].

In order to appreciate the relative contribution of heave acceleration and surge to the very large bending response encountered above, the dynamic response under appropriate variations of the above excitation condition is simulated and is summarized in Table 4. Excitation A is defined in Table 3 and excitation condition B is same as excitation A except that the surge amplitude is reduced to one half, $S_o = 0.75m$. Excitation condition C involves only the current and heave motion of excitation A. In all above simulations, a drag coefficient $C_d = 1.2$ has been used. Although not presened here because of limitation of space, the shape of the maximum axial stress for excitations B and C are very similar to the above Figures for excitation A indicating that heave acceleration is the predominant factor in determining the character of the maximum axial stress.

Table 4 Effect of heave and surge on the response of riser A

Max. stresses (*MPa*)	Condition A	Condition B	Condition C
Tension	136	140	119
Bending	−533	−487	−402
Total axial	−538	−491	−403

It should be pointed out that maximum tension stress occours at a different time instant than maximum bending and total axial stress as before. As can be seen from Table 4, the maximum total axial stress is primarily due to bending and the contribution from negative tension is very small. In addition, the effect of direct lateral loading from different surge amplitudes to the maximum total axial stress is much smaller than the direct effect of heave acceleration and the resulting effective compression of the riser for part of the period of oscillation. This indicates that the predominant phenomenon in determining the maximum total axial stress is heave induced dynamic buckling.

6. Compliant Hang-off

Since the maximum stresses obtained under rigid hang-off are very large, compliant hang-off is introduced in order to reduce tension variation. The tensioner is designed so that no extensional natural frequencies are in the range of substantial wave excitation and so that adequate available tensioner stroke is obtained[1,29]. The tensioner gas mean pressure is chosen so as to statically center the riser top end near the middle of the slip joint stroke. The value of the spring constant of the tensioner chosen is 14.2 *KN/m*. The first two extensional natural frequencies under compliant hang-off are 0.13 *rad/s* and 5.30 *rad/s*, which are away from significant direct wave excitation. A simple one degree freedom analysis predicts that the tension variation under this compliant hang-off can be kept within 10% of the static tension. As expected this hang-off mode provides compliance between the surface support vessel and the riser system, thereby, keeping tension variation small. Figure 7 is the plot of maximum total axial stress along the length encountered in one period of excitation and shows significant reduction of maximum stress from higher than 500*MPa* to less than 100*MPa*. Figures 8 to 11 are plots of tension and bending stresses along the length for different instances within one period of oscillation and indicate that tension variation remains small

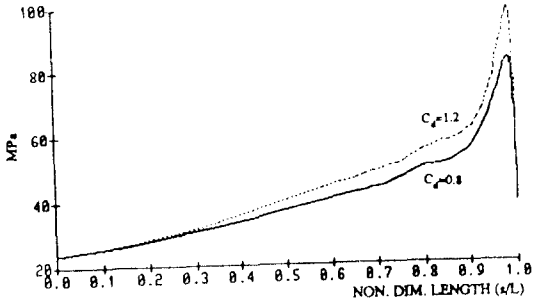

Fig. 7 Max. total axial stress uuder compliant hang-off

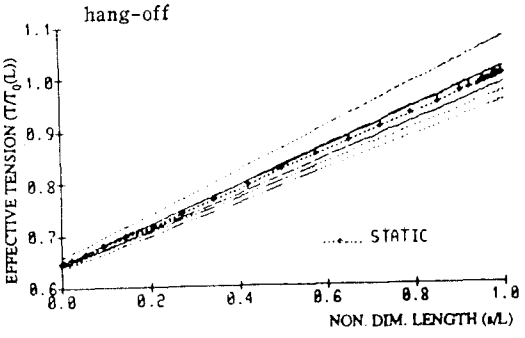

Fig. 8 Effective tension($C_d = 0.8$) under compliant hang-off

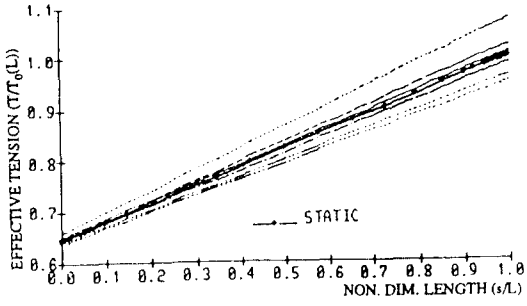

Fig. 9 Effective tension($C_d = 1.2$) under compliant hang-off

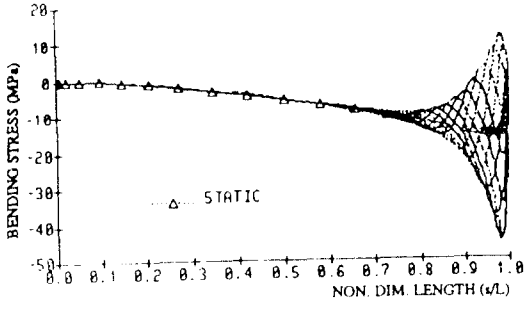

Fig. 10 Bending stress($C_d = 0.8$) under compliant hang-off

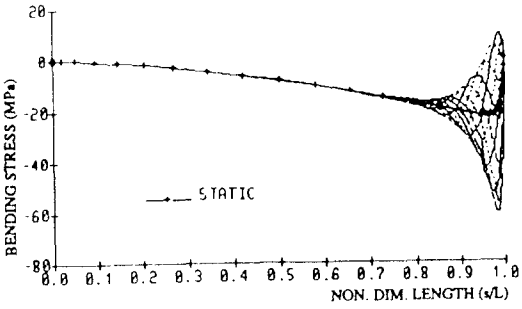

Fig. 11 Bending stress($C_d = 1.2$) under compliant hang-off

and that negative total tension is avoided. As a result, bending stresses are reduced to an acceptable range.

In Ref. (29), additional examples for longer risers may be found. In addition to the phenomena illustrated above, such longer under rigid hang-off also experience extensional resonance which is significant because of the small damping associated with axial vibrations. Extensional resonance, by itself, also leads to significant dynamic tension, even when the heave amplitude is very small, and affects the dynamic buckling response of the riser. The compliant hang-off concept was found to also be beneficial in this case.

7. Conclusions and Recommendations

The maximum bending stress under rigid hang-off is primarily due to effective compression which, in turn, is due to downward heave acceleration. Lateral loading (e.g. surge and direct wave and current loading), even in extreme excitation conditions, plays a smaller role in the maximum axial stress as compared to the effects of heave acceleration. The oscillatory stresses encountered in the rigid hang-off mode are significant and may lead to short term fatigue failure. Compliant hang-off reduces tension variation to a small fraction of static tension and, as a result, improves the level of bending response of the hanging riser system.

Based on the results of this work, the following

recommendations for further research may be made. The response of the riser to random excitation under rigid and compliant hang-off should be studied in the time domain using a non-linear three dimensional model of the riser behavior. In such a simulation, the first and second order vertical and horizontal support platform motions to a wave spectrum should be employed. Field verification of the benefits arising from the proposed compliant hang-off as compared to rigid hang-off is recommended. In particular, such experiments may provide better estimates of damping forces particularly important near extensional resonance. Such estimates are important for very deep water applications[25,29]. Finally, the vibration isolation concept studied in this paper in connection with hanging risers may also prove useful in the design of other ocean systems such as deep ocean mining pipes, flexible risers etc.

Acknowledgments

Funding for this research was obtained from the M. I. T. Sea Grant College Program. The second author was also supported by Daewoo Shipbuilding & Heavy Machinery Co. during his stay at M. I. T., where the above research was conducted.

References

1) Azpiazu, W. R. and V. N. Nguyen, "Vertical Dynamics of Marine Risers", Offshore Technology Conference(OTC4378), pp. 243-249, May, 1984

2) Bliea, A., "Dynamic Analysis of Single Span Cables", PhD thesis, Massachusetts Institute of Technology, 1984

3) Burgess, J. J., "Natural Modes and Impulsive Motions of a Horizontal Shallow Sag Cable", PhD thesis, Masschusetts Institute of Technology, 1985

4) Chung, J. S., A. K. Whitny, and W. A. Londen, "Non-Linear Transient Motion of Deep Ocean Mining Pipe", Offshore Technology Conference(OTC 3832), May, 1980

5) Crandall, S. H., et al., "Dynamics of Mechanical and Electromechanical System", McGraw Hill, 1968

6) Ferziger, J. H., "Numerical Methods for Engineering Application", Wiley, 1981

7) Garrett, D. L., "Dynamic Analysis of Slender Rods", Transaction of the ASME, Journal of Energy Resources Technology (104), Dec., 1982

8) Gottlieb, D. and S. A. Orszag, "Numerical Analysis of Spectral Method; Theory and Applications", SIAM, Philadelphia, Pensylvania, 1977

9) Hoerner, S. F., "Fluid Dynamic Drag", Hoerner, 1965

10) Hsu, C. S., "The Response of a Parametrically Excited Hanging String in Fluide", Journal of Sound and Vibration 39(3), 1975

11) Kim, Y. C., "Nonlinear Vibration of long Slender Beams", PhD thesis, Massachusetts Institute of Technology, 1983

12) Landau, L. D., "Theory of Elasticity", Pergamon Press, 1970

13) Love, A. E. H., "A Treatise on the Mathematical Theory of Elasticity", Dover, 1944

14) McNamara, J. F. and S. Giloy, "Non-Linear Dynamics of Disconnected Marine Risers", Proceedings of 4th International Offshore Mechanics and Arctic Engineering Symposium, 1985

15) NAG., "Numerical Algorithms Group Fortran Library", NAG, Oxford, England, 1987

16) Nordgren, R. P., "On Computation of the Motion of Elastic Rods", Journal of Applied Mechanics, Sep., 1974

17) Nordgren, R. P., "Dynamic Analysis of Marine Risers with Vortex Excitation", Journal of Energy Resources Technolgy ASME Trans. (104), pp. 14-19, 1982

18) Patel, M.H. and S. Sarohia, "Dynamic Response of Free Hanging Risers in Waves", Proceedings of the 3rd International Symposium on Offshore Mechanics and Arctic Engineering, ASME, New Orleans, Louisiana, 1984

19) Patrikalakis, N.M., Theoretical and Experimental Procedures for the Prediction of the Dynamic Behavior of Marine Riser", PhD thesis, Massachusetts Institute of Technology, 1983

20) Patrikalakis, N.M and C. Chryssostoimdis, "Vortex Induced Response of a Flexible Cylinder in a Constant Current", Journal of Energy Resources Technology, ASME Trans. (107), pp. 244-249, 1985

21) Patrikalakis, N.M., "Three Dimensional Compliant Riser Analysis", Proceedings of the 5th International Symposium on Offshore Mechanics and Arctic Engineering, Tokyo, Japan, ASME 3, pp. 458-465, April, 1986

22) Patrikalakis, N.M. and C. Chryssostomidis, "Vortex Induced Response of a Flexible Cylinders in a Sheared Current", Journal of Energy Resources Technology, ASME Trans, Vol. 108, pp. 59-64, 1986

23) Pereyra, V., "Codes for Boundary Value Problems in Ordinary Differential Equation", Springer-Verlag, 1979

24) Sarpkaya, T. and M. Isaacson, "Mechanics of Wave Forces on Offshores", Nostrand, 1981

25) Sparks, C.P., J.P. Cabillic, and J-C. Schawann, "Longitudinal Resonant Behavior of Very Deep Water Risers", Offshore Technology Conference(OTC 4738), pp. 201-211, May, 1982

26) Tikhonov, S. and V.K. Zubarev, "Simulation of Non-Linear Vibrations of an Elevating Pipeline", Offshore Technology Conference (OTC 4234), pp. 51-58, May, 1982

27) Triantafyllou, G. S., M.S., Triantafyllou, and C. Chryssostomidis, "On the Formation of Vortex Streets Behind Stationary Cylinders", Journal of Fluid Mechanics(170), 1986

28) Verley, R.L.P. and G. Moe, "The Forces on an Oscillating Cylinder in a Current", VHL Report (STF 60A79061), Sep., 1979

29) Yoon, D.Y., "An Investigation on the Behavior of Hanging Risers", PhD thesis, Massachusetts Institute of Technology, 1987